

# Characterization and Modeling of Visible Light Communication Channels

Ahmed Al-Kinani<sup>1</sup>, Cheng-Xiang Wang<sup>1</sup>, Harald Haas<sup>2</sup>, and Yang Yang<sup>3</sup>

<sup>1</sup>Institute of Sensors, Signals and Systems, School of Engineering & Physical Sciences, Heriot-Watt University, Edinburgh EH14 4AS, U.K.

<sup>2</sup>Institute of Digital Communications, School of Engineering, The University of Edinburgh, Edinburgh EH9 3JL, U.K.

<sup>3</sup>Shanghai Research Center for Wireless Communications (WiCO), Shanghai, 201210, China.

Email: {aa1304, cheng-xiang.wang}@hw.ac.uk, h.haas@ed.ac.uk, yang.yang@wico.sh

**Abstract**—The performance of visible light communication (VLC) system may potentially be degraded by wireless optical channel distortions resulting from path loss and temporal dispersions. In order to devise techniques to combat the effects of channel distortions, an accurate channel model is needed. In this paper, we propose a new field of view (FOV) geometry-based single bounce (GBSB) model for VLC channels. Statistical properties of the proposed GBSB model are then studied, such as the channel gain, mean excess delay, root mean square (RMS) delay spread, Rician factor, and time correlation. Also, the required illuminance for the proposed scenario and the number of light emitting diodes (LEDs) per LED lamp are estimated.

**Keywords**—Visible light communications, channel modeling, RMS delay spread, time correlation, illuminance.

## I. INTRODUCTION

VLC systems have recently attracted a considerable interest for indoor wireless data transmissions. They become one economical solution to address the spectrum scarcity problem in radio frequency (RF) wireless systems. Having the ability to provide illumination and communication at the same time, VLC has been considered as one of the most promising communication technologies for future wireless networks [1]. Compared with RF based communication systems, VLC systems have many attractive features such as use of unlicensed frequency bands, immunity to RF interference, no health concerns, and excellent security properties since wireless optical signals do not penetrate through walls. Besides, it is an energy-efficient and low-cost technology [1]. Obviously, VLC networks will not replace RF networks and instead they will coexist in order to provide ubiquitous coverage. VLC systems utilize off-the-shelf incoherent white LEDs (WLEDs) as signal transmitters and p-intrinsic-n (PIN) photodiodes (PDs) or avalanche PDs (APDs) as signal receivers. Unlike in RF systems, in VLC systems the phase, frequency, and amplitude of the individual electromagnetic waves cannot be modulated. Therefore, information can be reliably encoded only in the signal intensity. Intensity modulation with direct detection (IM/DD) has been considered as the de-facto method of implementing optical wireless systems principally due to its reduced cost and complexity [2].

For VLC systems, channel characteristics depend on the type of environment, scatterers, and positions of the optical source and PD. Different wireless optical propagation environments or scenarios will cause different channel characteristics.

A considerable amount of work has been published in terms of channel characterization in the infrared spectrum, e.g., [3] and [4]. It is well known that VL and infrared bands exhibit different characteristics, which necessitates the development of VLC channel models. However, little attention has been given to the channel characterization and modeling in the VL spectrum. The authors in [5] and [6] investigated VLC channels using deterministic ray tracing approach based on Zemax. Indoor environment is subject to variations and hence indoor channel characteristics can change as a result of small movement of objects, furniture, and transmitter or receiver positions. In this paper, we derive a novel GBSB model for VLC channels. To the best of our knowledge, this is the first time that a GBSB model is proposed to model VLC channels.

The rest of this paper is organized as follows. Section II describes VLC propagation scenario. A FOV channel model is introduced in Section III. In Section IV, simulation results are presented. Conclusions are finally drawn in Section V.

## II. VLC PROPAGATION SCENARIO

In general, wireless optical link configuration can be classified according to: 1) the degree of directionality of optical source and receiver and 2) the existence of the line-of-sight (LoS) path between the optical source and receiver. Six link configurations and the trade-off between them are detailed in [4]. However, there are two basic link configuration schemes for indoor VLC systems, namely, the LoS and non-LoS (NLoS) configurations, which are both considered in this study. The proposed VLC propagation scenario can be illustrated in Fig. 1. VLC employs incoherent WLEDs used for solid-state lighting (SSL) as signal transmitters. Incoherent WLED lamps can increase coverage area and alleviate the need for alignment with receiver. WLED lamps usually consist of a significant number of single chips, each presenting an angular distribution following generalized Lambertian radiation pattern, which has uniaxial symmetry and is given as [3]

$$R(\alpha^T) = \frac{m+1}{2\pi} \cos^m(\alpha^T), \alpha^T \in [-\pi/2, \pi/2]. \quad (1)$$

Here,  $\alpha^T$  is the angle of irradiance which is commonly denoted as the angle of departure (AoD) and  $m$  is mode number of the radiation lobe, which specifies the directionality of the source. Mode number can be calculated as  $m = -\frac{0.693}{\ln(\cos(HP))}$  [3], where  $HP$  is half power emission angle of the LED, i.e., the

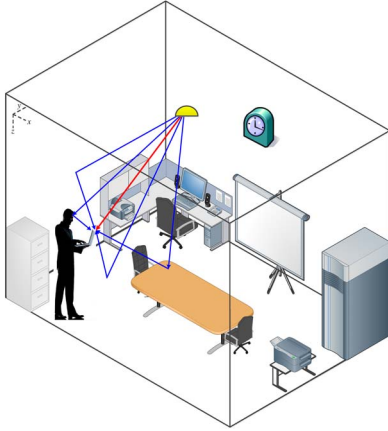


Fig. 1: VLC Propagation Scenario.

view angle when radiant intensity is half of the value at  $0^\circ$ . Most of LEDs have  $HP = 60^\circ$ , i.e.,  $m=1$  [7]. At the receiving side, the PD is modelled as an active area  $A_R$  collecting the radiation incident at angle  $\alpha^R$  smaller than the PD FoV. Only rays that incident within receiver's FoV will be captured. Incidence angle is commonly denoted as the angle of arrival (AoA). The wireless optical channel gain at the receiving side is proportional to the square of the distance between the optical source and the PD (the inverse square law), and to the effective collection area of the PD  $A_{R_{eff}}$ , which is given as [3]

$$A_{R_{eff}} = \begin{cases} A_R \cos(\alpha^R), & 0 \leq \alpha^R \leq FoV \\ 0, & \alpha^R > FoV. \end{cases} \quad (2)$$

The PD can be integrated with end user device such as laptop, tablets, or smart phones as shown in Fig. 1. At the same time, we need to fulfil the lighting function. Lighting systems are most effectively designed based on the illuminance (light level) required by the tasks performed within specific space. The illuminance of a surface is the amount of light energy received per second per unit surface area. The SI unit of illuminance is lux (lx) and it is given as [10]

$$E = \frac{I(\alpha^T)}{r^2} \quad (3)$$

where  $I(\alpha^T)$  is luminous intensity, in unit of candela (cd). Luminous intensity of an optical source in a given direction is defined as the luminous flux per unit solid angle in that direction. Since LEDs presenting an angular distribution following generalized Lambertian radiation pattern (non-isotropic source of light), the luminous intensity is given as [10]

$$I(\alpha^T) = I(0)R(\alpha^T) \quad (4)$$

where  $I(0)$  is the center luminous intensity of an LED and it is provided by the manufacturers.

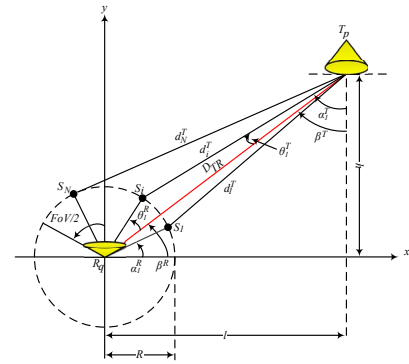


Fig. 2: FOV Model.

### III. VLC CHANNEL MODEL

#### A. The Geometrical FOV Model

In this section, we describe the proposed FOV-GBSB model for VLC channels. Fig. 2 illustrates the geometry of the proposed FOV-GBSB. This model is modified from the well-known one-ring model, which was first introduced in [8]. Let us now consider a general narrowband optical wireless system where the transmitter is WLED lamp which acts as fixed base station while the receiver is a PD acts as end user device. Each transmitted wave is further assumed to be scattered (reflected) only once. The FOV model is appropriate for describing environments, in which the base station is elevated and unobstructed, whereas the receiver is surrounded by a large number of local scatterers  $S_n(n = 1, 2, \dots, N)$ . In case if the LoS link is interrupted, the receiver will receive signals from different directions determined only by the distribution of the local scatterers. In FOV model, the local scatterers are distributed along the arc, with radius  $R$ , centred on the receiver. In this case the FoV of the PD sets the arc boundary. The distance between WLED lamp and the receiver is denoted by  $D_{TR}$ , while the distance between the  $n$ th transmitted light ray and  $n$ th local scatterer  $S_n$  is denoted by  $d_n^T$ . AoD of the  $n$ th transmitted light ray is denoted by  $\alpha_n^T$ , and the corresponding AoA is described by  $\alpha_n^R$  ( $n = 1, 2, \dots, N$ ).

#### B. The Reference Model of FOV VLC Channel Model

In the proposed model, the LoS component of the channel impulse response (CIR) is deterministic and given as [4]

$$h_{T_p-R_q}^{LoS} = \frac{A_R}{\pi(D_{TR})^2} \cos^m(\alpha^T) \cos(\alpha^R). \quad (5)$$

In order to derive the reference model from the geometrical model shown in Fig. 2, we suppose a situation in which the  $n$ th light ray emitted from the LED lamp travels over  $S_n$  effective scatterers around the PD lying on an arc of radius  $R$  and impinge on the PD. The reference model is based on the assumption that the number of local scatterers is infinite  $S_n(n = 1, 2, \dots, \infty)$ . Consequently, the diffuse

component at the PD can be represented as a superposition of an infinite number of plane waves coming from different directions determined by the distribution of the local scatterers. Each scatterer  $S_n$  introduces a gain  $G_n$ . This parameter is dependent on the surface reflection coefficient  $\rho(\lambda)$  of the scatterer  $S_n$  and the direction of the  $n$ th incoming plane wave. To simplify the reference model, we assume that each scatterer  $S_n$  introduces an infinitesimal gain inversely proportional to the number of scatterers  $N$ , while directly proportional to the mean of reflection coefficient parameter  $\bar{\rho}(\lambda)$ . Hence,  $G_n$  can be expressed as  $G_n = \frac{\bar{\rho}(\lambda)}{N}$ .

For single bounce (SB) path  $(T_p - S_n - R_q)$ , CIR of the  $n$ th transmitted plane wave from optical source, interacting with the local scatterer  $S_n$ , and then arriving at the PD, can be written as

$$h_{T_p-S_n-R_q}^{SB} = \lim_{N \rightarrow \infty} \sum_{n=1}^N \frac{G_n A_R}{\pi(D_n^{TR})^2} \cos(\alpha_n^T)^m \cos(\alpha_n^R) \quad (6)$$

where  $D_n^T$  represents the total distance the  $n$ th ray travels from  $T_p$  via  $S_n$  to  $R_q$ . With the help of Fig. 2, the path lengths  $D_n^T$  can be expressed as  $D_n^T = d_n^T + R$ , where  $d_n^T$  can be determined by using the law of cosines as

$$d_n^T = \sqrt{R^2 + (D^{TR})^2 - 2RD^{TR} \cos(\theta_n^R)}. \quad (7)$$

Here,  $D^{TR}$  is the minimum distance that light can travel between optical source and the PD without interruption and  $\beta^R$  is the angle between  $D^{TR}$  and the PD plane.  $\beta^R$  is given as  $\beta^R = \sin^{-1}(\frac{h}{D^{TR}})$ , where  $h$  is the vertical distance between optical source and the PD. Hence,  $\theta_n^R$  can be written as  $\theta_n^R = \alpha_n^R - \beta^R$ . On the other hand, in optical source side, the corresponding angle  $\beta^T$  is given as  $\beta^T = \cos^{-1}(\frac{h}{D^{TR}})$ . We propose a new general method to derive the exact relationship between AoD and AoA for *FoV* scattering region. Applying the law of sines in the triangle  $T_p - S_n - R_q$  gives

$$\theta_n^T = \sin^{-1}\left[\frac{R \sin(\theta_n^R)}{d_n^T}\right]. \quad (8)$$

The AoD  $\alpha_n^T = \beta^T + \theta_n^T$ , where  $\beta^T$  and  $\theta_n^T$  are known as in above. Note that AoD  $\alpha_n^T$  and AoA  $\alpha_n^R$  are interdependent for single bounced rays. Hence, the wireless optical channel gain  $T_p - S_n - R_q$  of the reference model describing the link from the LED lamp to the PD can be expressed as

$$h_{T_p-S_n-R_q}^{SB} = \lim_{N \rightarrow \infty} \sum_{n=1}^N \frac{G_n A_R}{\pi(D_n^{TR})^2} \cos(\alpha_n^R) \cos(\beta^T + \theta_n^T)^m. \quad (9)$$

It is important to recall that the last term in (9) is a function of the AoA  $\alpha_n^R$  at the PD.

### C. The Simulation Model of *FOV* VLC Channel Model

In this step, a simulation model is derived from the reference model simply by replacing the infinite number of scatterers by a finite number  $N$ . The reasonable value for the number of discrete scatterers  $N$  is in the range from 40 to 50 [9].

On the other hand, the proper values for the model parameter  $\alpha_n^R$  can be obtained by modifying extended method of exact Doppler spread (EMEDS) used in [9] to fit *FOV* model. This method assuming that scatters are uniformly distributed around the receiver. Modified EMEDS produces a set of discrete AoAs  $\{\alpha_n^R\}_{n=1}^N$  given as

$$\alpha_n^R = \frac{\pi}{N}(n - \frac{1}{2}) + \alpha_0^R, \quad n = 1, 2, 3, \dots, N \quad (10)$$

where  $\alpha_0^R$  is called the angle-of-rotation. The EMEDS reveals its best performance if the angle-of-rotation  $\alpha_0^R$  is defined as

$$\alpha_0^R = \frac{\alpha_n^R - \alpha_{n-1}^R}{4} = \frac{\pi}{4N}. \quad (11)$$

## IV. RESULTS AND ANALYSIS

In performing simulations, entries of environmental parameters are summarized in Table I.

TABLE I: Link parameters used in computer simulations.

<b>Room Parameters</b>	
Width (W)	5m
Length (L)	5m
Height (H)	3m
Reflection Coefficient ( $\bar{\rho}(\lambda)$ )	0.8
<b>Optical Source Parameters</b>	
Mode Number ( $m$ )	1
Coordinates (x,y,z)	2.55 2.55 3
<b>Photodiode Parameters</b>	
Area	1cm <sup>2</sup>
Field of view ( <i>FoV</i> )	80°
<b>Other Parameters</b>	
Number of Scatterers	40
Arc Radius	0.5m

### A. Environment Illuminance

By substituting (1) and (4) in (3), illuminance can be rewritten as

$$E = I(0) \frac{m+1}{2\pi r^2} \cos^m(\alpha^T). \quad (12)$$

Current office operations primarily involve computer based, mobile phones, tablets and high quality printed paper-reading tasks. For such environment and in accordance with the lighting standard [11], a 200-800 lx span is suitable to illuminate the environment presented in Fig. 1. The illumination was assessed at 1 m above the floor. Simulation results of applying (12) illustrate how the whole environment can be illuminated with brightness within standard levels as shown in Fig. 3. Theoretically, based on above illumination distribution we can estimate the number of LED chips that uniformly distributed per lamp. It is shown that we need for 1000 LED chips of maximum luminous intensity of 10 cd and half-intensity radiation angle of 120° (commercially available LED chip) [12]. This figure is comparable to the results in [13].

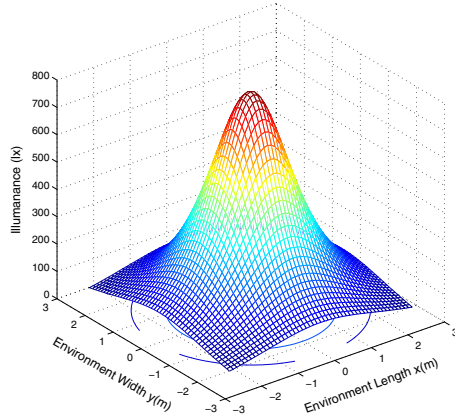


Fig. 3: Illuminance ( $I_x$ ) of a LoS link for optical source located at (2.55,2.55,3).

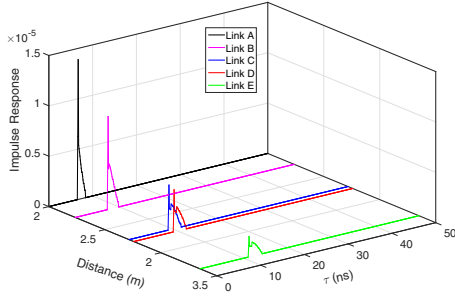


Fig. 4: SB CIR for links A, B, C, D, and E.

### B. VL Channel Characteristics

1) *VL CIR* : The CIR of the LoS component is deterministic and can be expressed in (5). The number of partitions is set to 50 with special resolution 0.1 m and temporal resolution 0.5 ns. Result shows visible light CIR of 7.9577e-06 at a 2 m distance compared to infrared CIR of 1.2318e-06 at a 3.9051 m in configuration (A) in [4]. Regarding to SB, the CIR of five links (A, B, C, D and E) with different PD positions are shown in Fig. 4. PD coordinates are given in Table II. These coordinates represent the most probable positions for the optical receiver. It is clear that the VL channel can be characterized (under specific reflection coefficient assumption) firstly by the distance between the optical source and the PD and secondly by the AoA with respect to the normal on the PD surface where higher channel response at shorter optical path and smaller AoA. The power is seen to decrease for SB impulse responses; however, they tend to add to a significant amount for total power as shown in Fig. 4. Furthermore, SB power arrives much later than that from LoS component. Fig. 5 illustrates the behaviour of distance and AoA with respect to the optical source and the PD locations for proposed model.

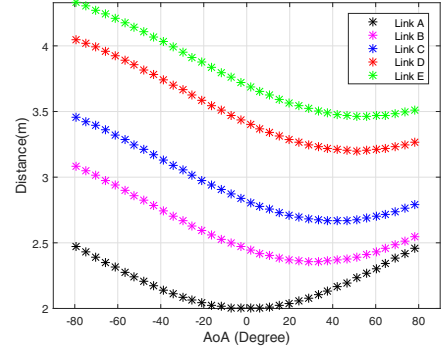


Fig. 5: AoA and Distance behaviour for links A, B, C, D and E.

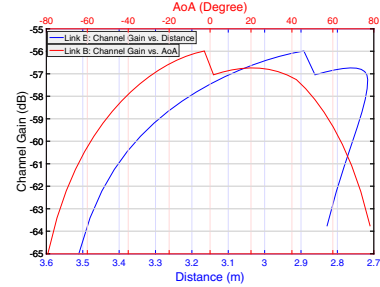


Fig. 6: Channel gain for link B with respect to AoA and path distance.

2) *Channel DC gain  $H(0)$* : The optical power loss is expressed by the channel DC gain, which is given as [2]

$$H(0) = \int_{-\infty}^{\infty} h(t) dt. \quad (13)$$

Channel DC gain in db is related to the received power in dBW when 1 W is transmitted [14]. Fig. 6 shows the channel gain for link B with respect to path distance and AoA. It is clear that higher gain can be obtained at AoA closer to the normal to the detector plane and at shorter path.

3) *Delay Spread*: One of important features of a wireless optical multipath channel is that the channel stretches the transmitted signal in time what is known as temporal dispersion. Any delay measured longer than the delay corresponds to the arrival of the first transmitted signal at the receiver is called an excess delay  $\tau_i$ . Temporal dispersion can be quantified by the channel RMS delay spread ( $\sigma_\tau$ ) [2]

$$\sigma_\tau = \sqrt{\frac{\sum_i (\tau_i - \mu_\tau)^2 h_i^2}{\sum_i h_i^2}} \quad (14)$$

where  $\mu_\tau$  is the mean excess delay and is given as

$$\mu_\tau = \frac{\sum_i \tau_i h_i^2}{\sum_i h_i^2}. \quad (15)$$

RMS delay spread is critical in high-speed applications, where the maximum bit rate is  $R_b \leq 1/10\sigma_\tau$  [15]. Conse-

quently, this will set the limit on the symbol length that can be used in order to avoid intersymbol interference (ISI). Notice that the delay spread would still be nearly zero as long as the LoS path dominates. However, the spread increases as receiver locations move away from the room center (since optical source located at room center).

4) *Rician Factor*  $K_{\text{rf}}$ : We still assume the transmitted power is 1 W. The power ratio between the LoS and SB links can be quantified by the Rician factor :  $K_{\text{rf}} = \frac{P_{\text{LoS}}}{P_{\text{SB}}}$  [2].

All the above fundamental channel characteristics for links A, B, C, D and E are presented in Table II. We can see the effect of the position of receiver and transmitter with respect to each other in terms of path distance and AoA. For example, if the receiver has been moved from the room centre (Link A) to the corner (link E), the channel gain and Rician factor will remarkably decrease, while path distances and hence RMS delay spread will increase. Furthermore, as a comparison between Link (A) and configuration (A) in [4], we can notice that Rician factor is comparable in both.

TABLE II: VLC Channel Characteristics.

Link	Distance (m)	PD (x,y)	Channel Characteristics			
			$H(0)$	$\mu_\tau$ (ns)	$\sigma_\tau$ (ns)	$K_{\text{rf}}$
A	2.0000	2.55,2.55	1.412e-04	6.9166	0.2954	2.2546
B	2.3585	2.55,3.80	0.864e-04	8.3316	0.5048	1.9059
C	2.6693	3.80,3.80	0.594e-04	9.5229	0.5979	1.6881
D	2.8284	0.55,2.55	0.499e-04	10.1223	0.6313	1.5943
E	3.4641	0.55,0.55	0.272e-04	12.4610	0.7136	1.3003

### C. Wireless Optical Channel Time Correlation

Time autocorrelation function (ACF) for the LoS link is given as [9]

$$r_{h_{pq}}(\Delta t) = E[h_{pq}^{\text{LoS}}(t)h_{pq}^{*\text{LoS}}(t + \Delta t)] \quad (16)$$

where  $E[\cdot]$  is the statistical expectation operator. Assuming that the user is moving at 8.0m/s, Fig. (7) clearly depicts that the correlation properties vary significantly for different delays especially when the PD is located at the corner.

## V. CONCLUSIONS

In this paper, we have proposed a novel FOV GBSB model for VLC channels. It has been shown that the channel gain, delay spread, and Rician factor (under specific reflection coefficient assumption) of the proposed model depend on the AoA and the distance between the optical source and the PD. Our results have further pointed out that wireless optical channel is highly correlated at the centre of the environment and the correlation is decreasing gradually when moving away towards the environment edges.

## ACKNOWLEDGEMENT

The authors gratefully acknowledge the support of this work from the EU H2020 5G Wireless project (No. 641985), EU FP7 QUICK project (No. PIRSES-GA-2013-612652), 863 Project in 5G (No. 2014AA01A707), National Science and

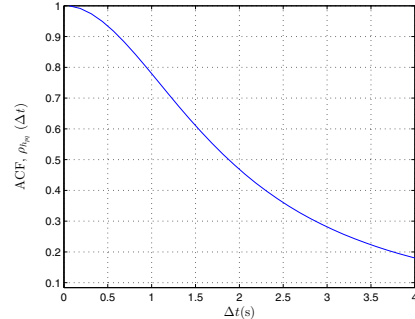


Fig. 7: Time ACF of the LoS link.

Technology Major Project (No. 2014ZX03003012-001), and National Natural Science Foundation of China through the Major International Joint Research Project (No. 61210002).

## REFERENCES

- [1] C.-X. Wang et al., "Cellular architecture and key technologies for 5G wireless communication networks," *IEEE Commun. Mag.*, vol. 52, no. 2, pp. 122-130, Feb. 2014.
- [2] Z. Ghassemlooy, W. Popoola, and S. Rajbhandari, *Optical Wireless Communications: System and Channel Modelling with MATLAB*, 1st ed, CRC press, NY, USA, 2013.
- [3] F. R. Gfeller and U. H. Bapst, "Wireless in-house data communication via diffuse infrared radiation," *Proc. IEEE*, vol. 67, no. 11, pp. 1474-1486, Nov. 1979.
- [4] J.R. Barry, J.M. Kahn, W.J. Krause, E.A. Lee and D.G. Messerschmitt, "Simulation of multipath impulse response for indoor wireless optical channels," *IEEE JSAC*, vol. 11, no. 3, pp. 367-379, Apr. 1993.
- [5] E. Sarbazi, M. Uysal, M. Abdallah and K. Qaraqe, "Indoor channel modelling and characterization for visible light communications," in *Proc. ICTON14*, Graz, Austria, July 2014, pp.1-4.
- [6] F. Miramirkhani, M. Uysal and, E. Panayircib, "Novel channel models for visible light communications," in *Proc. SPIE15*, San Francisco, California, United States, Feb. 2015.
- [7] O. Bouchet, *Wireless Optical Communications*, London: UK, 2012.
- [8] D. S. Shiu, G. J. Foschini, M. J. Gans, and J. M. Kahn, "Fading correlation and its effects on the capacity of multielement antenna systems," *IEEE Trans. Commun.*, vol. 48, no. 3, pp. 502-513, Mar. 2000.
- [9] M. Pätzold, *Mobile Radio Channels*, 2nd ed, John Wiley & Sons, United Kingdom, 2012.
- [10] R. R. Dudeja, *Pearson Guide to Objective Physics For Iit-Jee*, Dorling Kindersley, India, 2007.
- [11] METREL, *The Illuminance Handbook*. Slovenia, 2002, Code No. 20 750 690.
- [12] www.hebeiltd.com.cn (model S12NW6C)
- [13] J. Grubor et al., "High-speed wireless indoor communication via visible light," in *Proc. ITG'07*, Berlin, Germany, March 2007.
- [14] J. B. Carruthers and S. M. Carroll, "Statistical impulse response models for indoor optical wireless channels," *International J. Commun. Systems*, vol. 18, pp. 267-284, April 2005.
- [15] D. Wu, Z. Ghassemlooy, S. Rajbhandari, and H. Le Minh, "Improvement of the transmission bandwidth for indoor optical wireless communication systems using a diffused Gaussian beam," *IEEE Commun. Letters*, vol. 16, no. 8, pp. 1316-1319, Aug. 2012.